# Phenanthrenyl-indole as a fluorescent probe for peptides and lipid membranes

**Bruno F. Hermenegildo,[a] Goreti Pereira,[b] Ana S. Abreu,[a,b] Elisabete M. S. Castanheira,[a,*] Paula M. T. Ferreira,[b] and Maria-João R. P. Queiroz[b]**

[a] *Centro de Física (CFUM), Universidade do Minho, Campus de Gualtar, 4710-057 Braga, Portugal*

[b] *Centro de Química (CQ-UM), Universidade do Minho, Campus de Gualtar, 4710-057 Braga, Portugal*

**REVISED VERSION**

**Corresponding Author**:
E. M. S. Castanheira
Centro de Física, Universidade do Minho,
Campus de Gualtar, 4710-057 Braga, Portugal
Fax: +351 253604061
e-mail: ecoutinho@fisica.uminho.pt

**ABSTRACT**

A 3-(phenanthren-9-yl)-1*H*-indole-2-carboxylic acid (**2**) obtained from the cleavage of the methyl ester of the methyl 3-(phenanthren-9-yl)-1*H*-indole-2-carboxylate (**1**) was inserted into a peptide containing the RGD sequence. The GGRGDG peptide sequence was prepared by solid phase synthesis and coupled to compound (**2**), using diisopropylcarbodiimide (DIC) and 1-hydroxybenzotriazole (HOBt) in DMF. The peptide (**3**) labelled with the phenanthrenylindole moiety was obtained in 31% yield.

The photophysical properties of the phenanthrenyl-indole derivatives were studied in several solvents of different polarity. Compounds **1** and **2** have reasonably high fluorescence quantum yields (between 27% and 85%) in non-protic solvents, the methyl phenanthrenyl-indole-2-carboxylate **1** being the more fluorescent compound. The fluorescence emission of both compounds is sensitive to solvent, indicating that they are good candidates for fluorescent probes. Fluorescence emission measurements of the labelled peptide in solution showed a strong decrease of $\Phi_F$ value caused by the attachment of the Gly-Gly-Arg-Gly-Asp-Gly chain.

The phenanthrenyl-indoles **1** and **2** and the labelled peptide **3** were incorporated in liposomes of dipalmitoyl phosphatidylcholine (DPPC) and dipalmitoyl phosphatidylglycerol (DPPG) and mixtures of both lipids. Steady-state anisotropy measurements showed that compounds **1** and **2** are located inside the lipid bilayers and are able to report the transition between the gel and liquid-crystalline phases. The RGD labelled peptide locates mainly in the outer part of the vesicle interface. These results indicate that the phenanthrenyl-indole moiety may be used as a fluorescent probe for peptides and lipid membranes.

**KEYWORDS**: Phenanthrenyl-indole; RGD-peptide; Fluorescence; Lipid membranes

**ABBREVIATIONS.** DPPC (dipalmitoyl phosphatidylcholine), DPPG (dipalmitoyl phosphatidylglycerol), PC (phosphatidylcholine), PG (phosphatidylglycerol), G (glycine), R (arginine), D (aspartic acid).

## 1. INTRODUCTION

Fluorescence spectroscopy is widely used to study proteins and peptides, with the vast majority of studies making use of the naturally occurring fluorophores, tyrosine and tryptophan. However, there is considerable interest in the incorporation of novel fluorophores, because they can offer site specific probes and, in many cases, can be chosen to allow selective excitation and detection [1-2]. Fluorescent peptides form a new generation of analytical tools for visualizing intracellular processes and molecular interactions at the level of single cells [3-4]. The sequence arginine–glycine–aspartic acid (RGD) (Figure 1) is found in many extracellular matrix proteins and is responsible for their interaction with a class of cell receptors known as integrins. These receptors are involved in the regulation of cellular proliferation and apoptosis. In particularly the integrin $\alpha_v\beta_3$ is over-expressed in some tumour cells and has been implicated in essential processes in the growth of solid tumours and in the development of metastases [5-9].

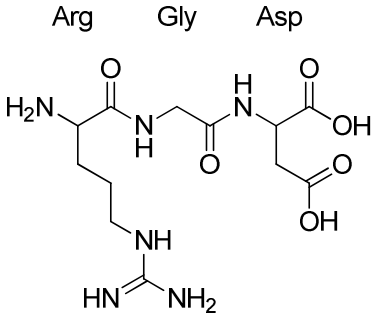


**Figure 1.** Tripeptide Arg-Gly-Asp.

In our laboratories we have been interested in the synthesis of new heterocyclic compounds that could be used as fluorescent probes for biological systems [10]. One of the strategies developed for the synthesis of these compounds involves the Suzuki-Miyaura cross-coupling of brominated dehydroamino acids with aryl boronic acids followed by a metal assisted C-N intramolecular cyclisation [11]. Using this methodology we were able to prepare a variety of indole derivatives and also to study their photophysical properties [10]. Among these compounds, the methyl 3-(phenanthren-9-yl)-1*H*-indole-2-carboxylate was prepared and showed to be a good candidate to be used as a fluorescence probe for biological systems [10c]. Continuing

this work, it was decided to link this compound to a peptide containing the arginine-glycine-aspartic acid (RGD) sequence.

The absorption and emission properties of the methyl 3-(phenanthren-9-yl)-1*H*-indole-2-carboxylate, 3-(phenanthren-9-yl)-1*H*-indole-2-carboxylic acid and of the labelled peptide were studied in both homogeneous solution and incorporated in lipid membranes of dipalmitoyl phosphatidylcholine and/or dipalmitoyl phosphatidylglycerol which are the main components of biological membranes.

## 2. EXPERIMENTAL

### Materials and Methods

Melting points (ºC) were determined in a Gallenkamp apparatus and are uncorrected. $^{1}H$ and $^{13}C$ NMR spectra were recorded on a Bruker Avance III at 400 and 100.6 MHz, respectively. $^{1}H$-$^{1}H$ spin-spin decoupling and DEPT θ 45º were used. HMQC and HMBC were used to attribute some signals. Chemical shifts are given in ppm and coupling constants in Hz. HRMS data were recorded by the mass spectrometry service of the University of Vigo, Spain.

All the solutions were prepared using spectroscopic grade solvents and ultrapure water (Milli-Q grade). 1,2-Dipalmitoyl-*sn*-glycero-3-phosphocholine (DPPC) and 1,2-Dipalmitoyl-*sn*-glycero-3-[phospho-*rac*-(1-glycerol)] (sodium salt) (DPPG) were purchased from Sigma-Aldrich (lipid structures are shown below).

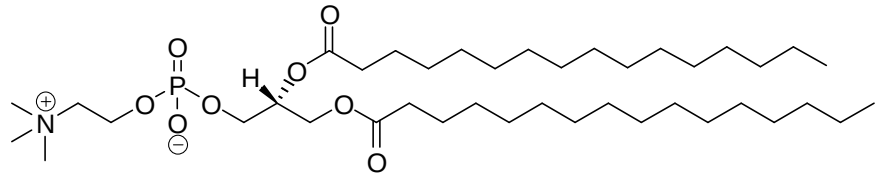

**DPPC**

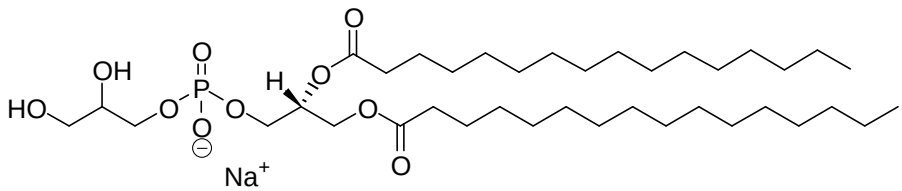

**DPPG**

For phospholipid vesicles preparation, the injection method was used [10b,12-14]. Defined volumes of stock solutions of lipid (50 mM in ethanol for DPPC and 13.4 mM in tetrahydrofuran for DPPG) and compounds **1** and **2** (0.197 mM for **1**, and 0.195 mM for **2**) were injected together at 60 ºC, well above the melting transition temperature of DPPC (*ca.* 41 ºC) [15] and DPPG (39.6 ºC) [16], under vigorous stirring, to an aqueous buffer solution (10 mM Tris-HCl, pH=7.2) also at 60 ºC. In all cases, the final lipid concentration was 1 mM, with compounds/lipid molar ratio of 1:500.

**Spectroscopic measurements**

Absorption spectra were recorded in a Shimadzu UV-3101PC UV-Vis-NIR spectrophotometer. Fluorescence measurements were performed using a Fluorolog 3 spectrofluorimeter, equipped with double monochromators in both excitation and emission, Glan-Thompson polarizers and a temperature controlled cuvette holder. Fluorescence spectra were corrected for the instrumental response of the system.

For fluorescence quantum yield determination, the solutions were previously bubbled for 40 minutes with ultrapure nitrogen. The fluorescence quantum yields ($\Phi_s$) were determined using the standard method (equation 1) [17,18]. 9,10-diphenylanthracene in ethanol ($\Phi_r$ = 0.95 [19]) was used as reference.

$$\Phi_s = \frac{A_r F_s n_s^2}{A_s F_r n_r^2} \Phi_r \qquad (1)$$

where *A* is the absorbance at the excitation wavelength, *F* the integrated emission area and *n* the refraction index of the solvents used. Subscripts refer to the reference (r) or sample (s) compound. The absorbance value at excitation wavelength was always less than 0.1, in order to avoid inner filter effects.

Solvatochromic shifts were described by the Lippert-Mataga equation (2), which relates the energy difference between absorption and emission maxima to the orientation polarizability, [20,21]

$$\bar{\nu}_{abs} - \bar{\nu}_{fl} = \frac{1}{4\pi\varepsilon_0} \frac{2\Delta\mu^2}{hcR^3} \Delta f + const \qquad (2)$$

where $\bar{\nu}_{abs}$ is the wavenumber of maximum absorption, $\bar{\nu}_{fl}$ is the wavenumber of maximum emission, $\Delta\mu = \mu_e - \mu_g$ is the difference in the dipole moment of solute molecule between excited ($\mu_e$) and ground ($\mu_g$) states, *R* is the cavity radius

(considering the fluorophore a point dipole at the center of a spherical cavity immersed in the homogeneous solvent), and $\Delta f$ is the orientation polarizability given by (eq. 3):

$$\Delta f = \frac{\varepsilon - 1}{2\varepsilon + 1} - \frac{n^2 - 1}{2n^2 + 1} \quad , \tag{3}$$

where ε is the static dielectric constant and *n* the refractive index of the solvent.

The steady-state fluorescence anisotropy, *r*, is calculated by

$$r = \frac{I_{VV} - G\, I_{VH}}{I_{VV} + 2G\, I_{VH}} \tag{4}$$

where $I_{VV}$ and $I_{VH}$ are the intensities of the emission spectra obtained with vertical and horizontal polarization, respectively (for vertically polarized excitation light), and $G = I_{HV} / I_{HH}$ is the instrument correction factor, where $I_{HV}$ and $I_{HH}$ are the emission intensities obtained with vertical and horizontal polarization (for horizontally polarized excitation light).

**Synthesis**

**Synthesis of the methyl 3-(phenanthren-9-yl)-1*H*-indole-2-carboxylate** (**1**): The synthesis of this compound was described elsewhere [10c].

**Synthesis of 3-(phenanthren-9-yl)-1*H*-indole-2-carboxylic acid (2**): A solution of NaOH 1M (3 equiv.) was added to a solution of **1** (0.6260 mmol; 0.220 g) in methanol (0.1 mol $dm^{-3}$) and the mixture was heated at reflux. When all the reagent had been consumed (4 h) the methanol was removed and the solution was acidified to pH 1-2 with HCl (5 mol.$dm^{-3}$). Filtration of the solid formed afforded compound **2** (0.200 g, 94%); m.p. 205-206 ºC. $^1$H NMR (400 MHz, $CDCl_3$): 7.09 (t, *J* = 6.8 Hz, 1 H, ArH), 7.29 (d, *J* = 8.4 Hz, 1 H, ArH), 7.36-7.45 (m, 3 H, ArH), 7.60-7.72 (m, 4 H, ArH), 7.79 (s, 1 H, ArH), 7.87 (d, *J* = 8.4 Hz, 1 H, ArH), 8.77 (t, *J* = 7.6 Hz, 2 H, ArH), 9.18 (br s, 1 H, NH) ppm. $^{13}$C NMR (100.6 MHz, $CDCl_3$): 111.91 (CH), 121.04 (CH), 122.20 (CH), 122.59 (CH), 122.73 (CH), 123.48 (C), 123.68 (C), 126.39 (CH), 126.46 (CH), 126.47 (CH), 126.68 (CH), 126.73 (CH), 126.84 (CH), 128.73 (CH), 129.06 (C), 129.16 (CH), 129.80 (C), 130.33 (C), 130.35 (C), 131.52 (C), 131.69 (C), 136.12 (C), 165.94

(C=O) ppm. HRMS (micrOTOF) [M+H]: calcd. for $C_{23}H_{15}NNaO_2$ 360.09950; found 360.09938.

**Synthesis of peptide** (**3**)**:** The GGRGDG peptide was prepared by solid phase synthesis using a Fmoc strategy. Fmoc-Gly-OH (1.2 equiv.) and diisopropylethylamine (DIPEA) (4 equiv. relative to the amino acid) in dry dichloromethane (DCM) were added to the 2-chlorotrityl chloride resin (0.5 g). The mixture was left stirring for 2h. At end of this time, the resin was washed with a mixture of DCM/MeOH/DIPEA (17:2:1) (3 × 20 mL), DMF (2 × 20 mL) and DCM (2 × 20 mL). The resin was dried in vacuum and the determination of the first residue attachment made by cleaving Fmoc with DBU and measuring the solution concentration of dibenzofulvene by UV spectroscopy. The loading amount was 0.58 $mol.g^{-1}$. After cleavage of the Fmoc group with a solution of piperidine in DMF, couplings were carried out using an excess of the Fmoc-amino acid (4 equiv., 1.20 mmol) with diisopropylcarbodiimide (DIC) and 1-hydroxybenzotriazole (HOBt) in DMF. Compound **2** (0.58 mmol, 195.6 mg) was coupled to the last amino acid using a similar stategy. The peptide labelled with the phenanthrenylindole was cleaved from the resin using a mixture of acetic acid/1,1,1-trifluoroethanol/DCM (2:2:6). The protecting groups were removed with TFA to give peptide **3** as a yellow solid (150.5 mg, 31 %). $^{1}$H NMR (400 MHz, DMSO-$d_6$): 11.97 (s, 1H, NH), 8.91 (t J=9.6 Hz, 1H, ArH), 8.64 (brs, 1H, NH), 8.30-8.20 (m, 4 H, ArH+NH), 8.14-7.87 (m, 5H, ArH+NH), 7.75-7.64 (m, 4H, ArH+NH), 7.59-7.46 (m, 3H, ArH+NH), 7.29-6.94 (m, 6H, ArH+$NH_3^+$), 4.59-4.56 (m, 1H, α-CH Asp), 4.28-4.22 (m, 1H, α-CH Arg), 3.84-3.61 (m, 8H, $CH_2$ Gly), 3.08-2.98 (m, 2H, δ-CH Arg), 2.67-2.52 (m, 2H, β-$CH_2$ Asp), 1.71-1.37 (m, 4H, β+γ $CH_2$ Arg). $^{13}$C NMR (400 MHz, DMSO-$d_6$): 24.77 ($CH_2$), 28.84 ($CH_2$), 36.36 ($CH_2$), 40.43 ($CH_2$), 40.35 ($CH_2$), 41.98 ($CH_2$), 42.08 ($CH_2$), 49.52 (CH), 52.43 (CH), 42.40 ($CH_2$), 112.50 (CH), 115.93 (C), 115.99 (C), 120.14 (CH), 120.33 (CH), 122.83 (CH), 123.21 (CH), 124.16 (CH), 126.50 (CH), 126.55 (CH), 126.66 (CH), 126.72 (CH), 126.91 (CH), 126.96 (CH), 128.70 (CH), 129.32 (CH), 129.80 (C), 130.09 (C), 130.29 (C), 131.35 (C), 131.43 (C), 135.51 (C), 166.53 (C=N), 168.52 (C=O), 168.68 (C=O), 168.77 (C=O), 170.92 (C=O), 170.98 (C=O), 171.04 (C=O), 171.75 (C=O), 171.84 (C=O). HRMS (micrOTOF) [M+H]: calcd. for $C_{41}H_{45}N_{10}O_{10}$ 837.33146; found 837.33039.

## 3. RESULTS AND DISCUSSION

### Synthesis

The methyl 3-(phenanthren-9-yl)-1*H*-indole-2-carboxylate (**1**) [10c] was prepared from a β-bromodehydrophenylalanine and 9-phenanthracenylboronic acid by a Suzuki-Miyaura cross-coupling followed by a Pd/Cu assisted C-N intramolecular cyclisation developed in our research group [10]. This compound was inserted into a peptide containing the RGD sequence after cleavage of the methyl ester (Scheme 1). Thus, compound **1** was treated with sodium hydroxide in methanol to afford the corresponding carboxylic acid (**2**) in a 94% yield. Compound **2** was conjugated with the hexapeptide glycine-glycine-arginine-glycine-aspartic acid-glycine (GGRGDG) synthesized by standard solid phase peptide synthesis (SPPS) using a fluorenylmethoxycarbonyl (Fmoc) protocol and a 2-chlorotrityl chloride resin. For side-chain protection the 2,2,4,6,7-pentamethyl dihydrobenzofuran-5-sulfonyl (Pbf) group for arginine and the *tert*-butyl ($^{t}$Bu) group for aspartic acid were used. Coupling reactions were performed with diisopropylcarbodiimide (DIC) and 1-hydroxybenzotriazole (HOBt). Compound **2** was coupled in solid phase using the same conditions. After cleavage from the resin and removal of the protecting groups, the labelled peptide **3** was obtained in 31% yield.

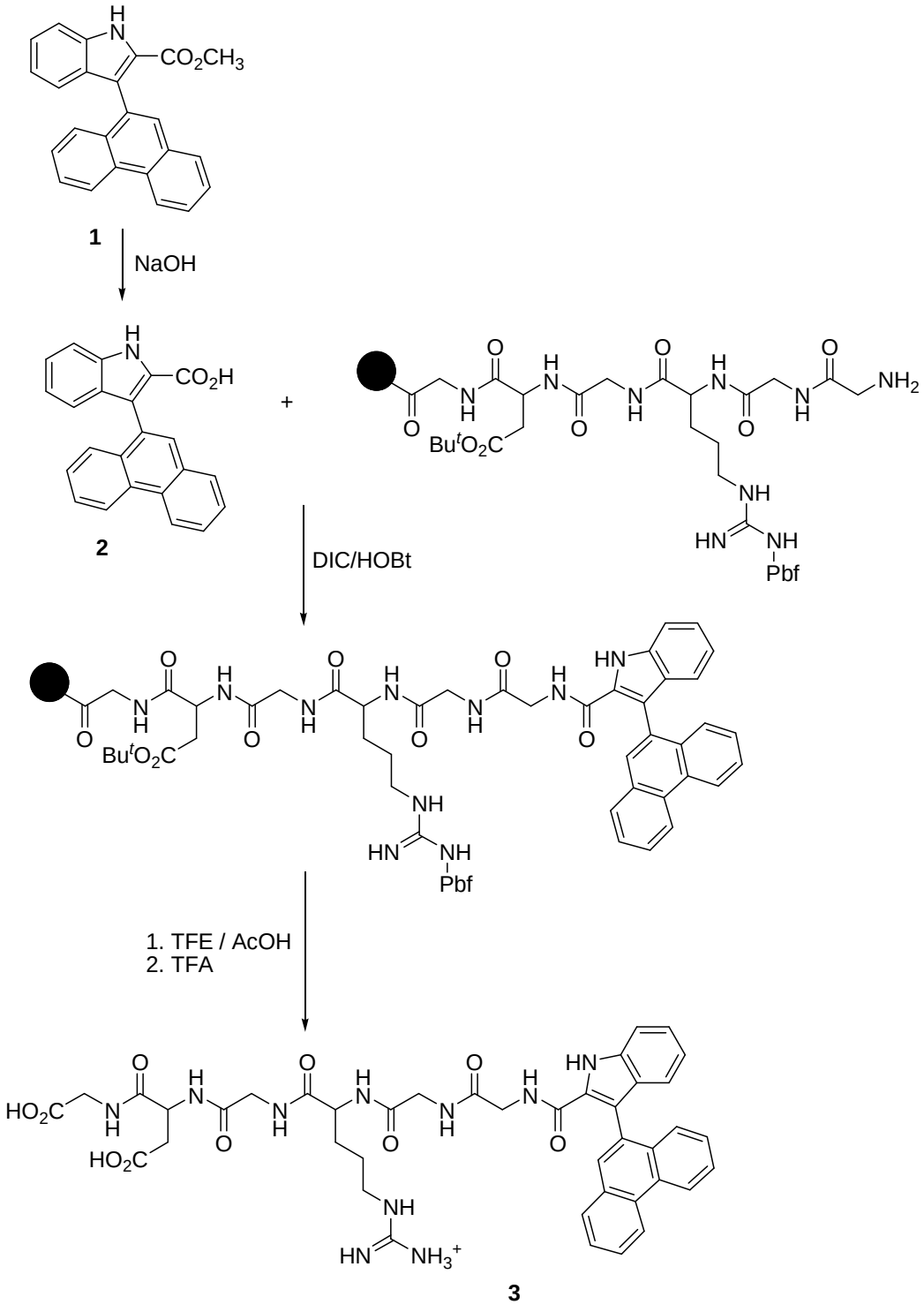


Scheme 1. Synthesis of compound **2** and peptide **3**.

## Fluorescence of compounds 1 and 2 in several solvents

The absorption and emission properties of compounds **1** and **2** were studied in ten solvents of different polarity. The maximum absorption ($\lambda_{abs}$) and emission wavelengths

($\lambda_{em}$), molar absorption coefficients (ε) and fluorescence quantum yields ($\Phi_F$) are presented in Table 1. The normalized fluorescence spectra of the phenanthrenyl-indoles **1** and **2** are shown in Figures 2 and 3, respectively. Examples of absorption spectra are shown as insets.

Table 1 – Maximum absorption ($\lambda_{abs}$) and emission wavelengths ($\lambda_{em}$), molar absorption coefficients (ε) and fluorescence quantum yields ($\Phi_F$) for compounds **1** and **2** in several solvents.

| **Solvent** | **$\lambda_{abs}$ (nm) (ε/$10^4$ $M^{-1}$ $cm^{-1}$)** | | **$\lambda_{em}$ (nm)** | | **$\Phi_F$ [a]** | |
|---|---|---|---|---|---|---|
| | **1** | **2** | **1** | **2** | **1** | **2** |
| Cyclohexane | 298 (2.47), 249 (6.27), 226 (5.14) | 297 (0.39) 252 (0.96) 226 (0.76) | 399 | 397 | 0.70 | 0.28 |
| Dioxane | 298 (2.85) 249 (6.97) 226 (6.23) | 298 (0.65) 249 (1.55) 227 (1.35) | 400 | 400 | 0.49 | 0.48 |
| Ethyl acetate | 297 (2.68) [b] | 297 (0.65) [b] | 400 | 403 | 0.85 | 0.33 |
| Dichloromethane | 298 (1.22) 249 (2.94) 226 (2.82) | 298 (0.51) 250 (1.22) 228 (1.03) | 404 | 410 | 0.80 | 0.34 |
| N,N-Dimethylformamide | 299 (2.71) [b] | 298 (0.57) [b] | 405 | 412 | 0.63 | 0.42 |
| Dimethylsulfoxide | 300 (2.61) [b] | 299 (0.64) [b] | 407 | 415 | 0.84 | 0.62 |
| Acetonitrile | 297 (2.25), 248 (5.88), 226 (4.64) | 297 (0.56) 248 (1.39) 225 (1.17) | 403 | 414 | 0.55 | 0.30 |
| Chloroform | 299 (2.58) [b] | 299 (0.69) [b] | 410 | 412 | 0.85 | 0.27 |
| Ethanol | 298 (2.47), 249 (6.26), 227 (4.84) | 298 (0.77) 248 (2.05) 225 (1.85) | 417 | 410 | 0.57 | 0.11 |
| Methanol | 297 (2.55) 248 (6.30) 226 (5.10) | 298 (0.63) 247 (1.73) 225 (1.78) | 422 | 412 | 0.52 | 0.07 |
| Water | 297 (0.42) 249 (0.75) 226 (0.80) | 298 (0.71) 251 (3.12) 225 (1.70) | 426 | 431 | 0.02 | 0.09 |

[a] Relative to 9,10-diphenylanthracene in ethanol ($\Phi_F$ = 0.95 at 25 ºC [19]). Error about 10%.

[b] *Solvents cut-off*: Dimethylsulfoxide: 270 nm; *N*,*N*-Dimethylformamide: 275 nm; Ethyl acetate: 265 nm; Chloroform: 250 nm.

In indole and its derivatives the near-ultraviolet absorption is generally attributed to two strongly overlapping $\pi \rightarrow \pi^*$ transitions [22-24], with an average ε value for non substituted indole of 5550 $M^{-1}$ $cm^{-1}$, which also justifies its relatively high fluorescence quantum yield [25]. Compound **1** presents high ε values ($\varepsilon > 1.2\times10^4$ $M^{-1}$ $cm^{-1}$) at the lowest energy maximum in all solvents studied, while for compound **2** the ε values are significantly lower ($\varepsilon \geq 3.9\times10^3$ $M^{-1}$ $cm^{-1}$) (Table 1). Many carbonyl compounds have a

low-lying $n \rightarrow \pi^*$ state, exhibiting low fluorescence quantum yields. As a carbonyl group is present in both compounds, the $\pi \rightarrow \pi^*$ and $n \rightarrow \pi^*$ electronic transitions can be nearby in energy, resulting in state-mixing [26]. The high values of the molar absorption coefficient for compound **1** can indicate a predominance of the $\pi \rightarrow \pi^*$ character, the latter being less pronounced for compound **2**.

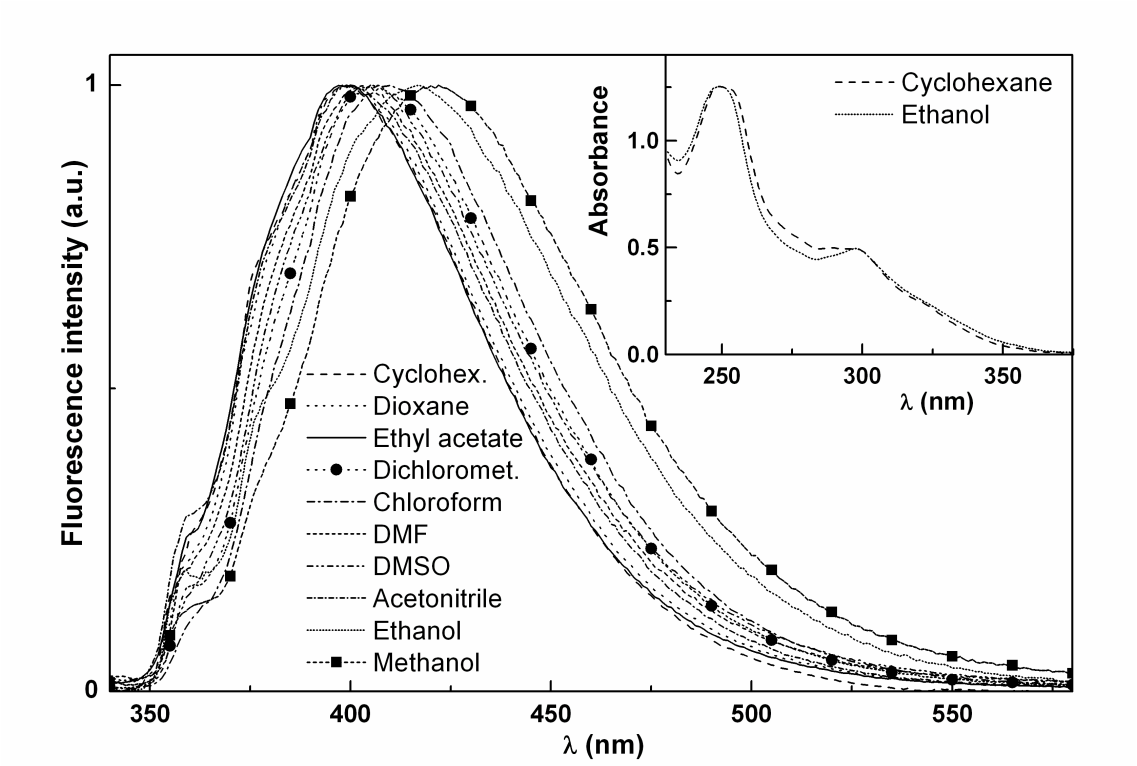


Figure 2. Normalized fluorescence spectra of $2 \times 10^{-6}$ M solutions of compound **1** in several solvents ($\lambda_{exc}$=325 nm). Inset: Absorption spectrum of $2 \times 10^{-5}$ M solutions of **1** in cyclohexane and ethanol, as examples.

For both compounds, significant red shifts are observed for emission in polar solvents, that are larger for compound **2**, if alcohols are not considered. In the absorption spectra, the red shifts are negligible (Table 1), indicating that solvent relaxation after photoexcitation plays an important role. In polar solvents, a clear band enlargement in emission is also observed (Figs. 2 and 3), which is usually related to an intramolecular charge transfer (ICT) mechanism and/or to specific solvent effects [20]. This behavior was already observed in other indole derivatives previously synthesized by us, namely the methyl 3-arylindole-2-carboxylates [27], the 1-heteroaryl-3*H*-benzothieno or

benzofuroindole-2-carboxylates [28], and several heteroaryl and heteroannulated indoles [29].

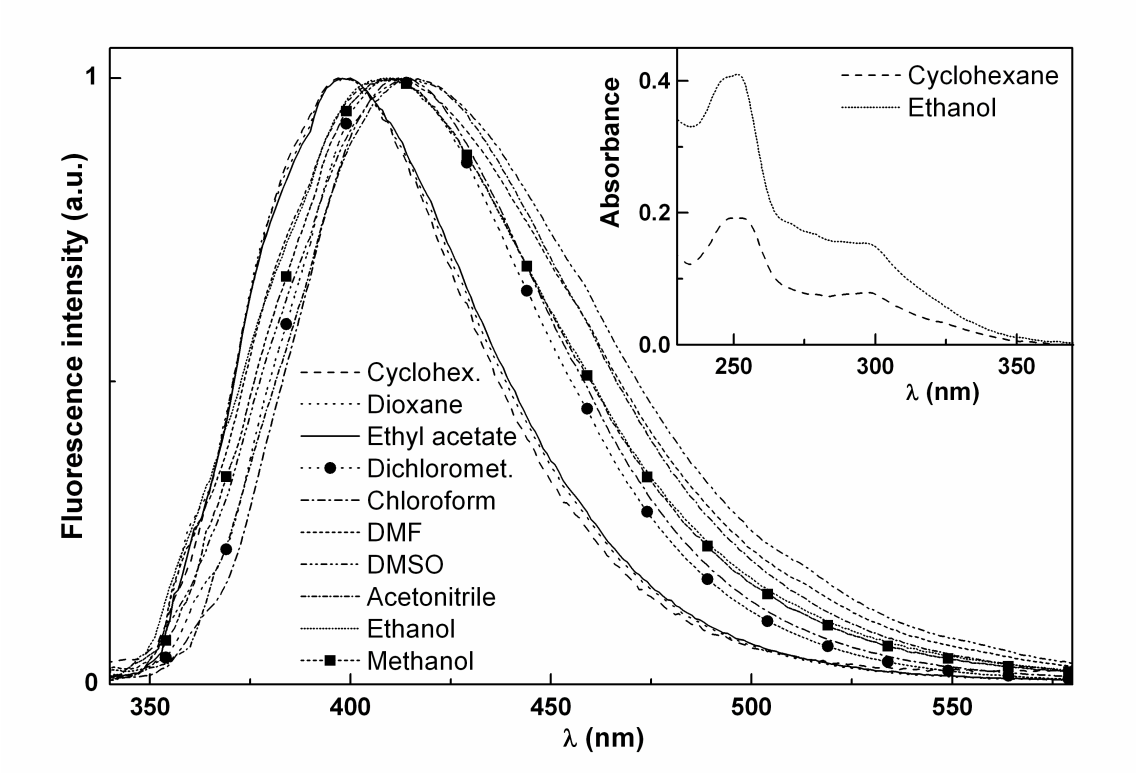


Figure 3. Normalized fluorescence spectra of $2\times10^{-6}$ M solutions of compound **2** in several solvents ($\lambda_{exc}$=325 nm). Inset: Absorption spectrum of $2\times10^{-5}$ M solutions of **2** in cyclohexane and ethanol, as examples.

The Lippert-Mataga plots for compounds **1**–**2**, shown in Figure 4, are reasonably linear in non-protic solvents, chloroform, alcohols and water exhibiting large positive deviations for the phenanthrenyl-indole **1**. This behaviour can be due to specific solute-solvent interactions by hydrogen bonds. Both compounds have the capability of hydrogen bonding formation through the NH group (donor) and the carbonyl group (acceptor). The formation of hydrogen bonds between chloroform and proton acceptors is known since a long time [31]. However, the Lippert-Mataga plot for compound **2** shows a small negative deviation for alcohols. One possible explanation for this fact could be the formation, in the ground state, of a hydrogen bond between the H atom of the carboxylic group and alcohols that becomes weaker in the excited state. The same behaviour does not occur in water, that exhibits a usual large positive deviation for both compounds (Figure 4). The generally larger solvatochromic shifts for compound **2** point

to a higher ICT character of the excited state for this compound, due to the presence of a carboxylic acid group.

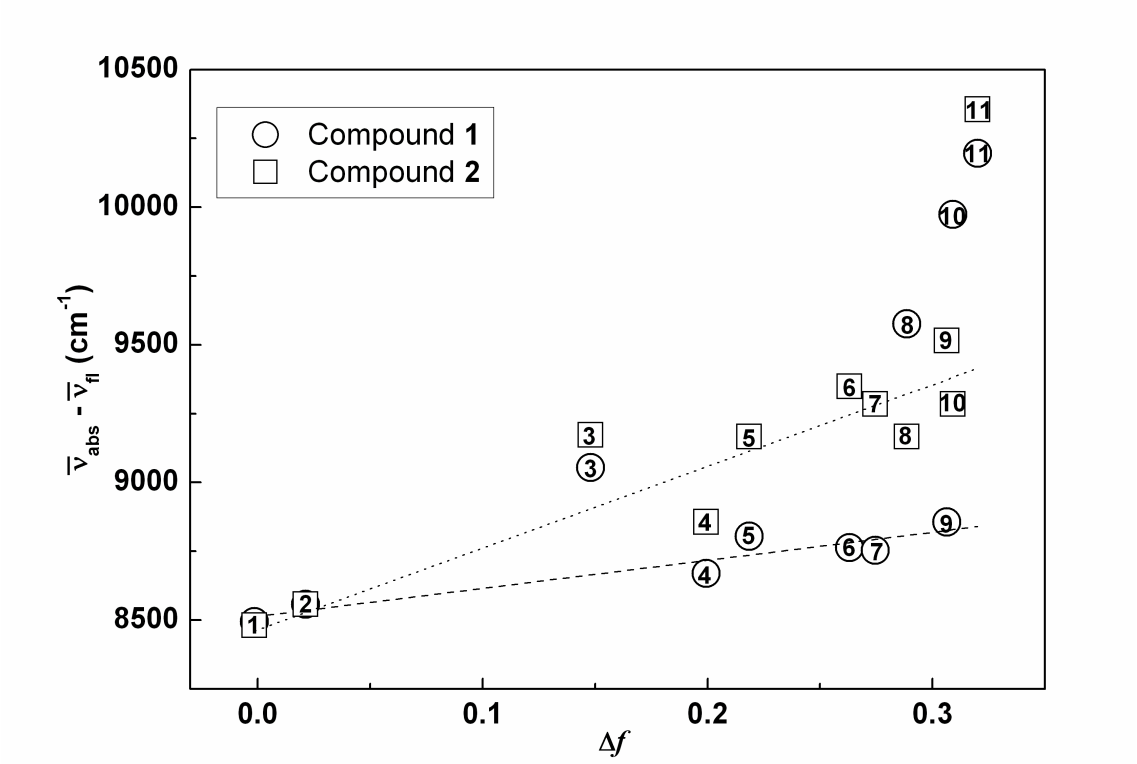


Figure 4. Lippert-Mataga plots for compounds **1** and **2**. Solvents: 1 - cyclohexane; 2 - dioxane; 3 - chloroform; 4 - ethyl acetate; 5 - dichloromethane; 6 - dimethylsulfoxide; 7 - *N*,*N*-dimethylformamide; 8 - ethanol; 9 - acetonitrile; 10 - methanol; 11 - water (values of ε and *n* were obtained from ref. [30]).

From *ab initio* molecular quantum chemistry calculations, obtained with Gaussian 09 software [32] and use of a 6-311+G(dp) basis set at the TD-SCF DFT (B3LYP) level of theory [33] in gas phase, the cavity radius (*R*) and the ground state dipole moment ($\mu_g$) were determined for the two compounds (Table 2). The optimized geometry of the ground state of phenanthrenyl-indoles **1** and **2** shows that the indole-2-carboxylate/carboxylic acid moiety is roughly perpendicular to the phenanthrene rings, while in the lower excited state a distortion occurs, with the approximation of the phenanthrenyl and indole moieties (Figure 5). The direction of the calculated dipole moments in the ground and excited state are also indicated.

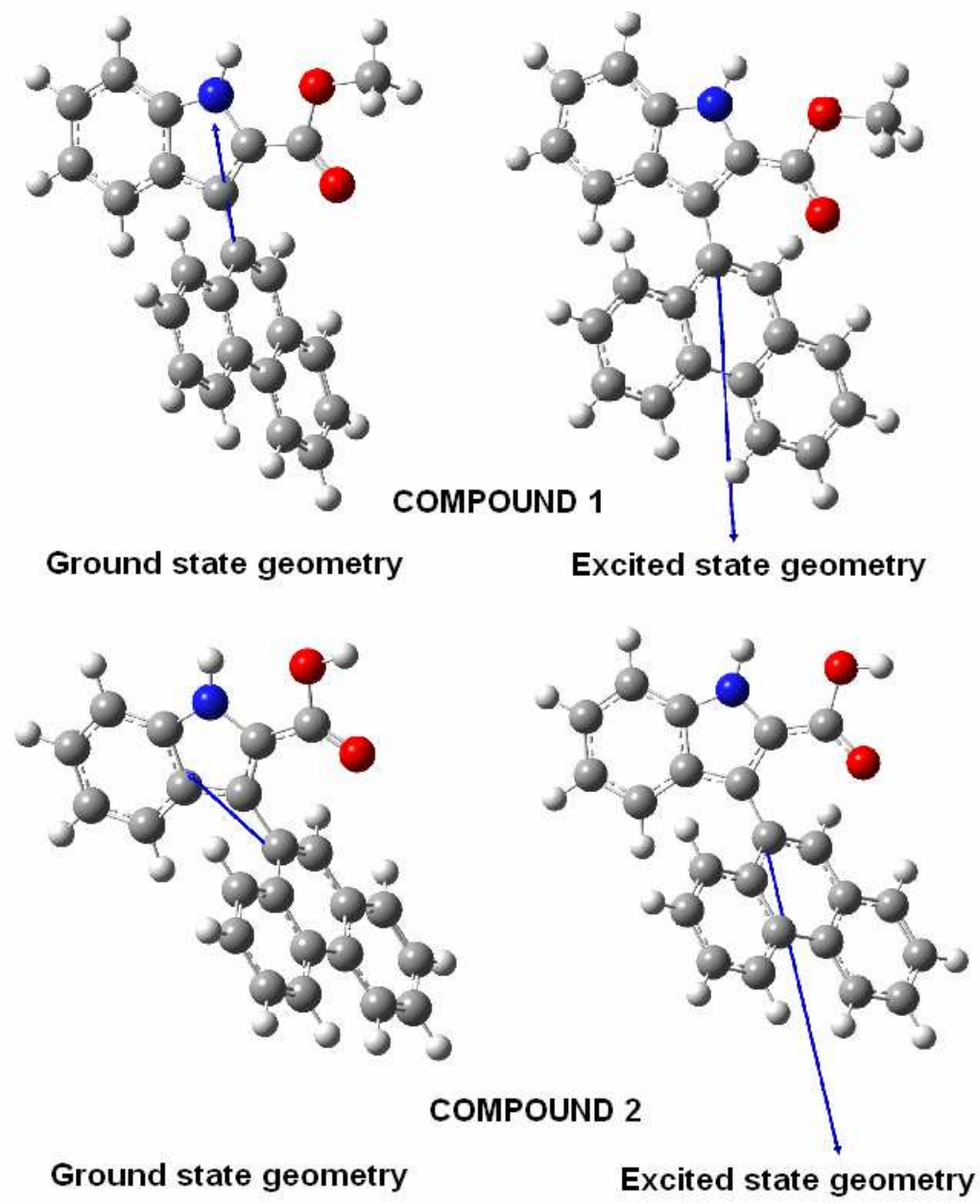


Figure 5. Optimized geometries of compounds **1** and **2** obtained by Gaussian 09 software (grey: C atoms; white: H atoms; red: O atoms; blue: N atoms). Left: ground state; Right: lowest excited singlet state. The arrows indicate the direction of the dipole moment.

The values of excited state dipole moments, estimated from the Lippert-Mataga plots and from molecular quantum mechanical calculations, are presented in Table 2. The values obtained from the calculations are slightly lower than the ones estimated from the Lippert-Mataga plots. Nevertheless, the $\mu_e$ values and the change in direction of the dipole moment (Figure 5) point to the presence of a significant charge transfer mechanism in the excited state, especially for the compound with the carboxylic group.

Table 2. Cavity radius (*R*) and ground state dipole moments ($\mu_g$), obtained from theoretical calculations, and excited state dipole moments ($\mu_e$) calculated from the Lippert-Mataga plots and from quantum mechanical calculations.

| Compound | Cavity radius, *R* (Å) | Ground state dipole moment, $\mu_g$ (D) | Excited state dipole moment, $\mu_e$ (D), from Lippert-Mataga plots | Excited state dipole moment, $\mu_e$ (D), from theoretical calculations |
|---|---|---|---|---|
| **1** | 5.7 | 2.81 | 7.2 | 6.9 |
| **2** | 5.6 | 2.53 | 10.0 | 8.1 |

Figure 6 displays the representation of HOMO and LUMO molecular orbitals for the two compounds, obtained with the calculated optimized geometries for ground and lowest excited singlet state. The HOMO molecular orbital is mainly located in the phenanthrenyl moiety, with a small contribution of the indole-2-carboxylate/carboxilic group, more significant for compound **1**. The HOMO-LUMO transition (for both geometries) of these phenanthrenyl-indoles shows an almost complete charge transfer from the phenanthrene rings to the indole-2-carboxylate/carboxylic moiety. This confirms the CT character of the excited state, more pronounced for compound **2**.

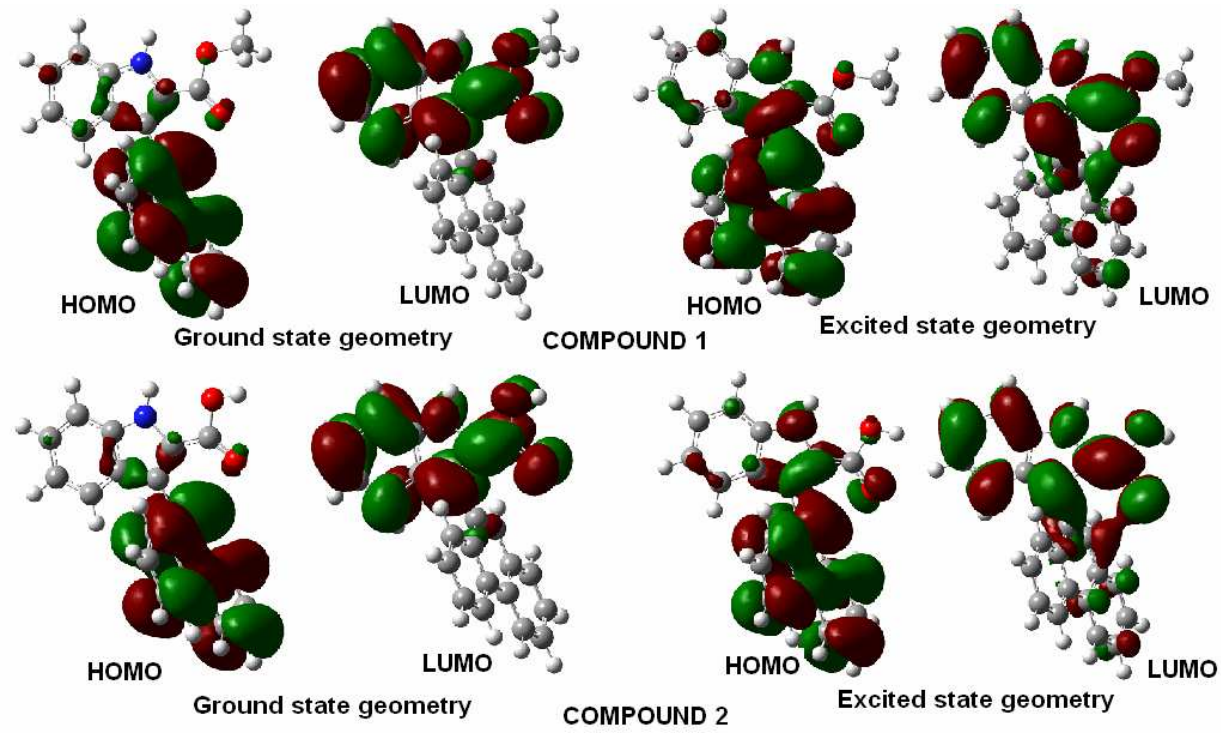


Figure 6. Representation of HOMO and LUMO molecular orbitals of the phenanthrenyl-indoles **1** (above) and **2** (below). Left: Optimized geometry for the ground state; Right: Optimized geometry for the lowest excited singlet state.

When in the excited state geometry, it is observed in LUMO molecular orbital of both compounds an additional electron density between the oxygen of the carbonyl group and a nearby double bond of the phenanthrenyl moiety. This is occurs as, due to the geometrical distortion, the distance between this oxygen atom and the C-C bond in the phenanthrenyl ring decreases from 3.7 Å to 2.7 Å.

Figure 7 shows the representation of the energy level diagram with the transition energies of both compounds. The mentioned additional electron density is probably responsible for the significant decrease in LUMO energy upon geometrical relaxation of the excited state. These results predict a large Stokes' shift that is, in fact, observed in the experimental data. The calculated absorption and emission transition energies are at lower energies than the ones experimentally observed. This can be due to solvent effects not accounted on the *ab initio* calculations as these were performed in the gas phase.

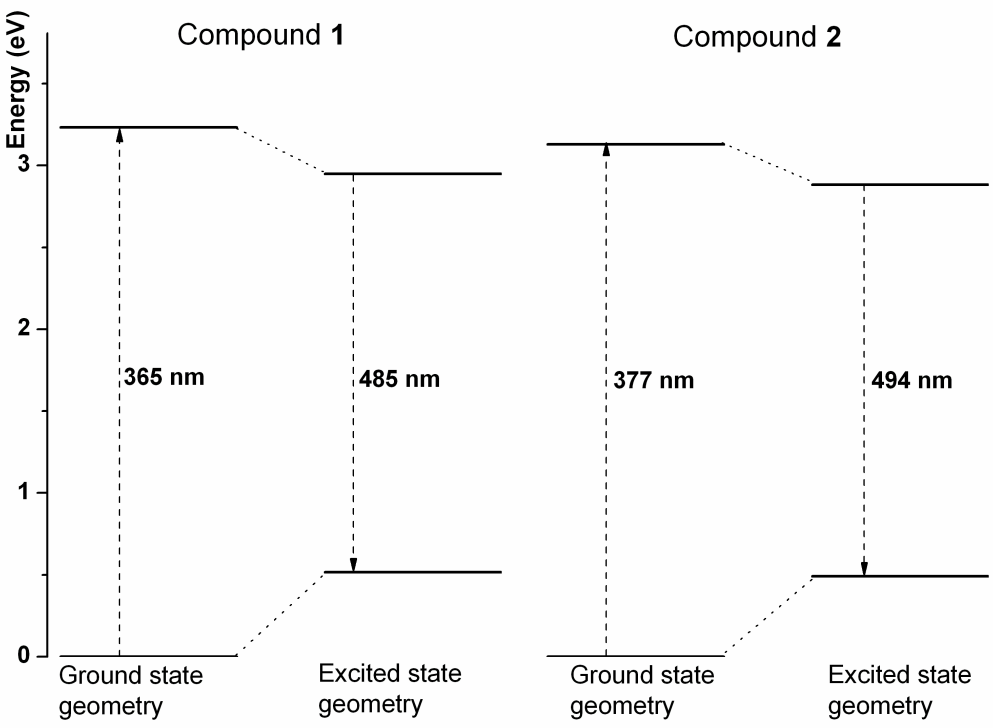


Figure 7. Representation of the energy level diagram, with the transition energies for both compounds, obtained by molecular quantum chemistry calculations.

Both compounds present reasonable to high fluorescence quantum yields in almost all solvents, compound **1** attaining 85% in some solvents (Table 1). A notable reduction of $\Phi_F$ is observed for compound **2** in alcohols, probably caused by an increase of singlet→triplet intersystem crossing efficiency through H-bond interaction.

The generally high fluorescence quantum yields and solvent sensitive emission of compounds **1** and **2** make them good candidates as fluorescence probes for biological membranes and proteins, as they can be excited without simultaneous excitation of tryptophan and other aromatic amino acids (tyrosine and phenylalanine) of proteins, which absorb light at $\lambda < 300$ nm [20].

**Fluorescence of peptide 3 in homogeneous solution**

Figure 8 shows the absorption (inset) and fluorescence spectra of the peptide **3** in ethanol and aqueous medium (pH = 7). A red shift (*ca.* 15 nm) and band enlargement is observed in aqueous media. Fluorescence quantum yields are presented in Table 3. It can be observed a strong fluorescence quenching of compound **1** caused by the attachment of a Gly-Gly-Arg-Gly-Asp-Gly chain. The high flexibility and length of the peptide chain leads to the increase of the non-radiative decay pathways (in particular, due to additional vibrational modes) and consequent decrease of $\Phi_F$ values.

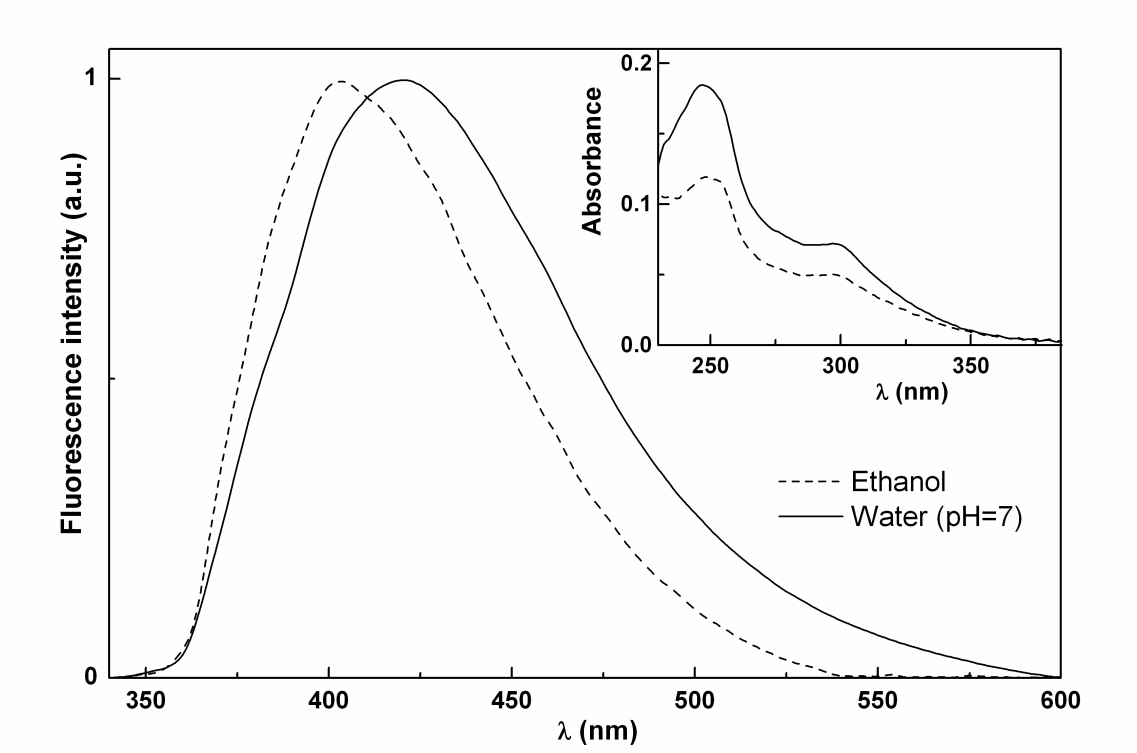


Figure 8. Normalized fluorescence spectra ($\lambda_{exc}$=325 nm) of $2\times10^{-6}$ M solutions of peptide **3** in ethanol and aqueous buffer (pH = 7). Absorption spectra of $2\times10^{-5}$ M solutions in the same solvents are shown as inset.

Table 3. Maximum absorption ($\lambda_{abs}$) and emission wavelengths ($\lambda_{em}$), molar absorption coefficients ($\varepsilon$) and fluorescence quantum yields ($\Phi_F$) for peptide **3**.

| **Solvent** | **$\lambda_{abs}$ (nm) ($\varepsilon/10^4$ $M^{-1}$ $cm^{-1}$)** | **$\lambda_{em}$ (nm)** | **$\Phi_F$ [a]** |
|---|---|---|---|
| Ethanol | 297 (0.25)<br>248 (0.60) | 404 | 0.075 |
| Aqueous buffer (pH =7) | 297 (0.36)<br>247 (0.92) | 423 | 0.038 [b] |

[a] Relative to 9,10-diphenylanthracene in ethanol ($\Phi$ = 0.95 [19])
[b] Non-deoxygenated solution.

A fluorescence study with variable pH (2–12) was also performed, to evaluate the potential of compound **1** to serve as fluorescent pH probe alone or when inserted in peptides. It was found that compound **1** alone presents a fluorescence emission insensible to pH (inset of figure 9). However, when linked to the peptide chain, significant variations in the fluorescence intensity can be detected (figure 9). Changes in the maximum emission wavelengths are negligible. The rise in the fluorescence intensity (inset of figure 9) starts at pH between 4 and 5. This variation can be related to the deprotonation of the side-chain carboxylic acid from the aspartic acid residue [34]. This could result in a hydrogen bond between the carboxylate anion and the indole group, affecting the peptide fluorescence quantum yield.

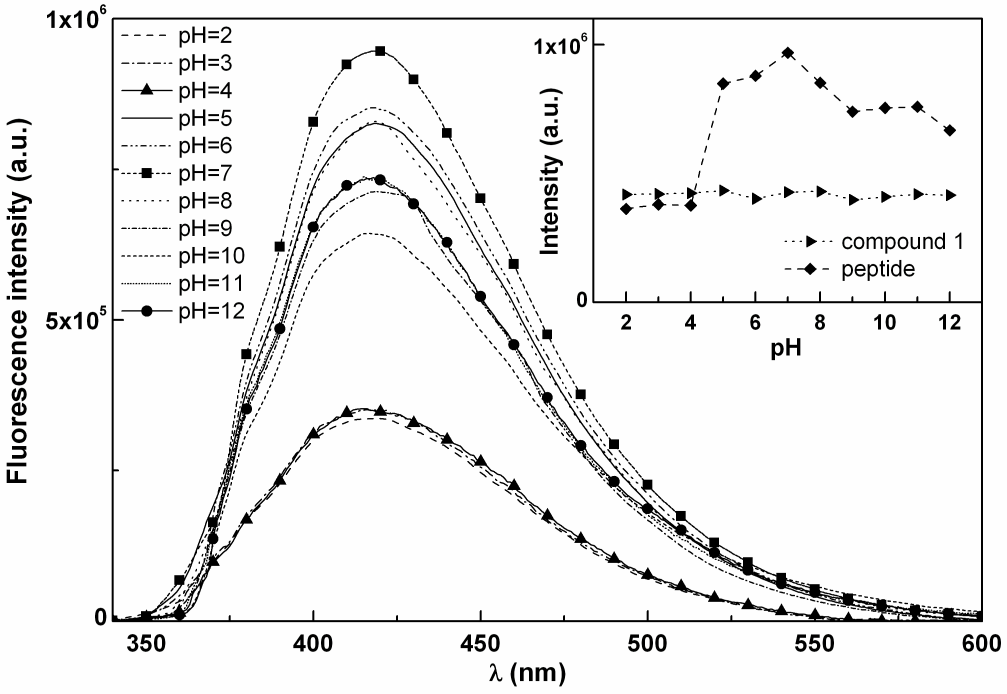


Figure 9. Fluorescence emission spectra ($\lambda_{exc}$=325 nm) of $1\times10^{-6}$ M solutions of peptide **3** in aqueous media of variable pH. Inset: Plots of emission intensity *vs.* pH for compound **1** alone ($1\times10^{-6}$ M) and linked to the peptide.

**Fluorescence of compounds 1-2 and peptide 3 in lipid membranes**

Photophysical studies of both compounds **1** and **2** and peptide **3** incorporated in lipid membranes composed of DPPC/DPPG mixtures were also performed. These two phospholipid molecules are the main components of biological membranes. It is known that, at room temperature, the neutral (zwitterionic) phospholipid DPPC (16:0 PC) and the anionic DPPG (16:0 PG) are in the ordered gel phase, where the hydrocarbon chains are fully extended and closely packed. Above the melting transition temperature, $T_m$= 41 ºC [15] for DPPC and $T_m$= 39.6 ºC [16] for DPPG, lipid chains attain the disordered and fluid liquid-crystalline phase.

The emission spectra of compounds **1** and **2** in lipid membranes of several DPPC/DPPG ratios at room temperature are displayed in Figure 10. At 55 ºC, the spectra in lipid membranes are very similar (data not shown) to those at lower temperature, with an expected fluorescence quenching (*ca*. 22% in neat DPPC and 45% in neat DPPG). In ethanol, the effect of increasing temperature (from 25 ºC to 55 ºC) in the fluorescence of these molecules is a ~ 42% reduction in intensity and a very small blue shift (1-2 nm for both compounds).

The fluorescence spectra in lipid membranes are similar for both compounds, displaying a red shift with increasing DPPG content in the lipid membrane (Figure 10 and Table 4). As the difference between DPPC and DPPG molecules is only the polar head group, these results point to a higher hydration level of these compounds in DPPG rich vesicles. Another possibility for this behavior is the occurrence of hydrogen bonding between the compounds and the OH groups of DPPG polar head.

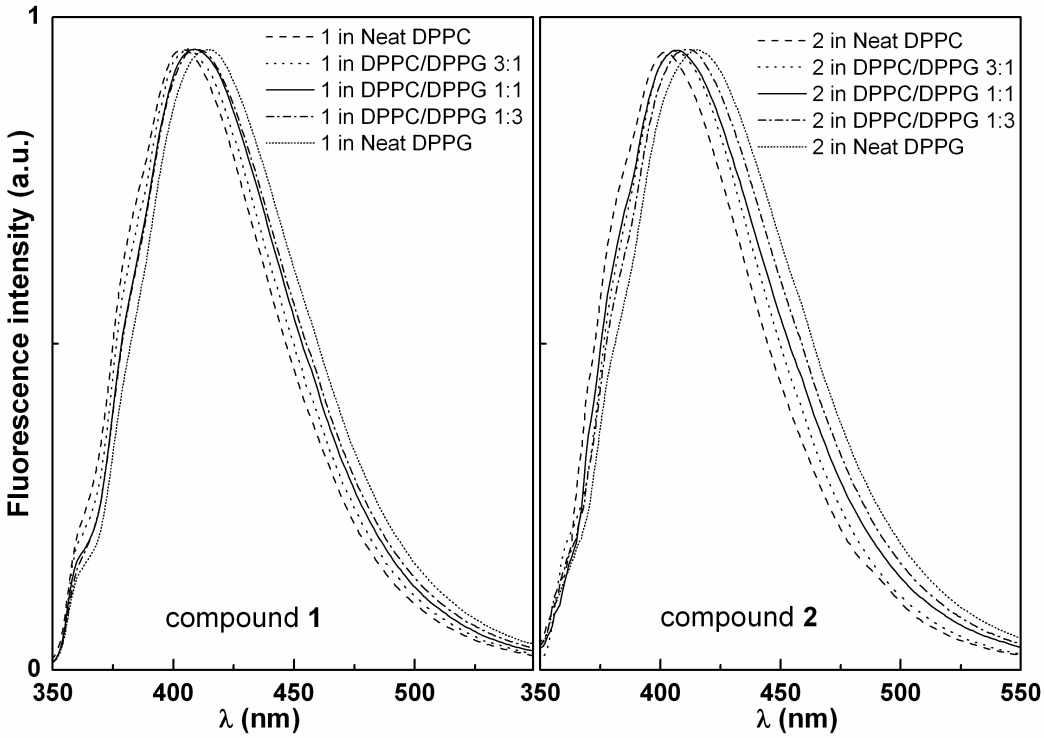


Figure 10. Normalized fluorescence spectra of compounds **1** and **2** ($2\times10^{-6}$ M) in lipid membranes of DPPC/DPPG ($\lambda_{exc}$=325 nm) at 25 ºC.

Fluorescence anisotropy measurements (equation 4) can give further information about these molecules behaviour in lipid membranes [35]. The fluorescence steady-state anisotropies determined for compounds **1** and **2** in lipid membranes of DPPC/DPPG are shown in Table 4. Anisotropy values in glycerol at room temperature were also determined for comparison, being similar for both molecules. The largest anisotropy values are observed in neat DPPC at gel phase (25 ºC), that exhibits a melting transition temperature higher than DPPG.

The fluorescence anisotropy values (Table 4) clear indicate that both compounds are mainly located inside the lipid bilayers. At 25 ºC (below the melting transition temperature of both lipids), the anisotropy of both molecules decreases monotonically with increasing DPPG content. The anisotropy values of both compounds are always higher in DPPC than in DPPG, the ratio $r_{DPPC}/r_{DPPG}$ attaining *ca.* 1.5 times at 25 ºC. Although DPPG molecules have a lower transition temperature, the difference between $T_m$ values of DPPC and DPPG is only 1.4 ºC. It is possible that some compound molecules are located in hydrated environments in DPPG, near the polar head groups,

justifying a further decrease in fluorescence anisotropy and the observed red shift in emission spectra. This behaviour is similar to that observed with a pyrenylindole-2-carboxylate [10b].

At 55 ºC, when both phospholipids are at the liquid-crystalline phase, the anisotropy values of both compounds exhibit a significant reduction in all the lipid membranes, showing that these indolic derivatives clearly detect the phospholipid gel to liquid-crystalline phase transition.

Peptide **3** was also incorporated in the same lipid membranes. The emission spectra at 25 ºC are presented in Figure 11 (the spectra at 55 ºC are similar in shape), and the fluorescence anisotropy values were also included in Table 4. Fluorescence spectra of **3** in lipid vesicles are clearly composed of two bands, one with maximum near 405 nm and another with maximum near 420 nm. Attaining to the spectra obtained in ethanol and in water (Figure 8 and Table 3), these two bands can correspond to two different locations in liposomes, one in the lipid bilayer probably near the polar phospholipids head groups, and another in highly hydrated environments. The fluorescence anisotropy of the peptide in lipid membranes is also wavelength dependent and the *r* values presented in Table 4 are average values.

Table 4. Steady-state fluorescence anisotropy (*r*) values and maximum emission wavelengths ($\lambda_{em}$) for compounds **1** and **2** and peptide **3** in mixed lipid membranes of DPPC/DPPG, below (25 ºC) and above (55 ºC) transition temperature of both lipids. Anisotropy values in glycerol at room temperature are also shown for comparison.

| **Lipid membrane composition** | **T (ºC)** | **1** | | **2** | | **Peptide 3** | |
|---|---|---|---|---|---|---|---|
| | | **$\lambda_{em}$ (nm)** | ***r*** | **$\lambda_{em}$ (nm)** | ***r*** | **$\lambda_{em}$ (nm)** | $\bar{r}$ |
| Neat DPPC | 25 | 405 | 0.147 | 403 | 0.164 | 405 | 0.093 |
| | 55 | 407 | 0.061 | 405 | 0.089 | 405, 425 *sh* | 0.064 |
| DPPC/DPPG 3:1 | 25 | 406 | 0.131 | 405 | 0.145 | 405 | 0.078 |
| | 55 | 408 | 0.061 | 407 | 0.078 | 406, 425 *sh* | 0.050 |
| DPPC/DPPG 1:1 | 25 | 409 | 0.127 | 407 | 0.124 | 406, 425 *sh* | 0.076 |
| | 55 | 410 | 0.056 | 409 | 0.073 | 407 *sh*, 425 | 0.043 |
| DPPC/DPPG 1:3 | 25 | 411 | 0.109 | 411 | 0.120 | 408 *sh*, 420 | 0.071 |
| | 55 | 410 | 0.045 | 413 | 0.062 | 408 *sh*, 420 | 0.040 |
| Neat DPPG | 25 | 414 | 0.087 | 415 | 0.107 | 412 | 0.063 |
| | 55 | 413 | 0.050 | 417 | 0.056 | 417 | 0.039 |
| Glycerol | 25 | 398 | 0.320 | 397 | 0.327 | 398 | 0.332 |

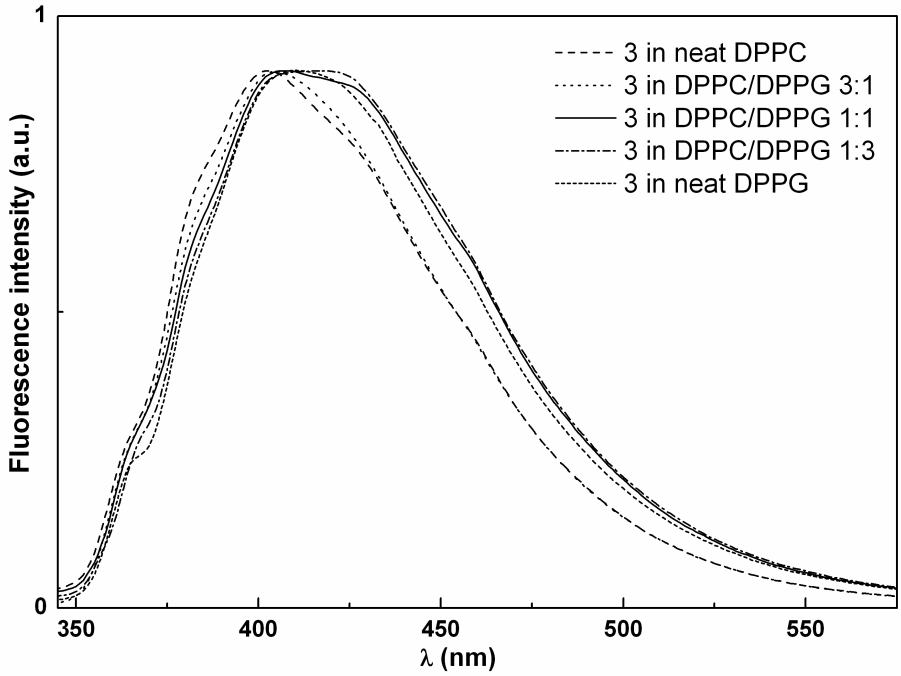


Figure 11. Normalized fluorescence spectra of peptide **3** ($2\times10^{-6}$ M) in lipid membranes of DPPC/DPPG ($\lambda_{exc}$=325 nm) at 25 ºC.

Due to this behaviour and considering the asymmetric nature of the peptide emission band (Figure 8), the fluorescence anisotropy components ($I_{VV}$ and $G\cdot I_{VH}$) were globally fitted to two sums of lognormal components (equations 5 and 6) [36], each sum characterized by a fitted anisotropy value, using a data analysis procedure previously developed by some of us [37],

$$I_{VV} = \sum_i \left(\frac{A_{1i}}{\left(\lambda - (\lambda_{max})_{1i} + a_{1i}\right)}\right) \exp\left(-c_{1i}^2\right) \exp\left\{-\frac{1}{2c_{1i}^2}\left[\ln\left(\frac{\lambda - (\lambda_{max})_{1i} + a_{1i}}{b_{1i}}\right)\right]^2\right\} + \\ + \sum_i \left(\frac{A_{2i}}{\left(\lambda - (\lambda_{max})_{2i} + a_{2i}\right)}\right) \exp\left(-c_{2i}^2\right) \exp\left\{-\frac{1}{2c_{2i}^2}\left[\ln\left(\frac{\lambda - (\lambda_{max})_{2i} + a_{2i}}{b_{2i}}\right)\right]^2\right\} \quad (5)$$

$$G \cdot I_{VH} = \sum_i \frac{A'_{1i}}{\left(\lambda - (\lambda_{max})_{1i} + a_{1i}\right)} \exp\left(-c_{1i}^2\right) \exp\left\{-\frac{1}{2c_{1i}^2}\left[\ln\left(\frac{\lambda - (\lambda_{max})_{1i} + a_{1i}}{b_{1i}}\right)\right]^2\right\} +$$
$$+ \sum_i \frac{A'_{2i}}{\left(\lambda - (\lambda_{max})_{2i} + a_{2i}\right)} \exp\left(-c_{2i}^2\right) \exp\left\{-\frac{1}{2c_{2i}^2}\left[\ln\left(\frac{\lambda - (\lambda_{max})_{2i} + a_{2i}}{b_{2i}}\right)\right]^2\right\} \quad , \quad (6)$$

where $A$ (or $A$') is the maximum intensity at wavelength $\lambda_{max}$ and the parameters $a$, $b$ and $c$ are given by [36]

$$c = \ln(\rho) / \sqrt{2\ln(2)} \qquad b = H \frac{\rho}{\rho^2 - 1} \exp\left(c^2\right) \qquad a = H \frac{\rho}{\rho^2 - 1} \quad (7)$$

where $H$ is the half-width of the band and ρ is the skewness. The lognormal function sums account for the vibrational structure of compound spectrum. The components (1 and 2) have two different fitted anisotropy values, $r_1$ and $r_2$, given by

$$r_1 = \frac{A_{1i} - A'_{1i}}{A_{1i} + 2A'_{1i}} \quad \text{and} \quad r_2 = \frac{A_{2i} - A'_{2i}}{A_{2i} + 2A'_{2i}} \quad , \quad (8)$$

due to the additivity law of anisotropy [35],

$$r = \sum_i \frac{I_i}{I_{total}} r_i \quad (9)$$

with
$$r_i = \frac{(I_i)_{VV} - G(I_i)_{VH}}{(I_i)_{VV} + 2G(I_i)_{VH}} \quad . \quad (10)$$

Therefore,

$$A'_{1i} = A_{1i}\left(\frac{1 - r_1}{1 + 2r_1}\right) \quad \text{and} \quad A'_{2i} = A_{2i}\left(\frac{1 - r_2}{1 + 2r_2}\right) \quad . \quad (11)$$

Figure 12 displays an example of the fit of anisotropy components, $I_{VV}$ and $G \cdot I_{VH}$ (equations 5 and 6), and the fitting to the anisotropy curve, as well as the respective spectral contributions recovered from the fitting. The results are given in Table 5. In all cases, two components were recovered, one with higher anisotropy ($r_1$) and lower maximum emission wavelength ($\lambda_{1,max}$) and another with higher emission wavelength ($\lambda_{2,max}$) and very low anisotropy value ($r_2$).

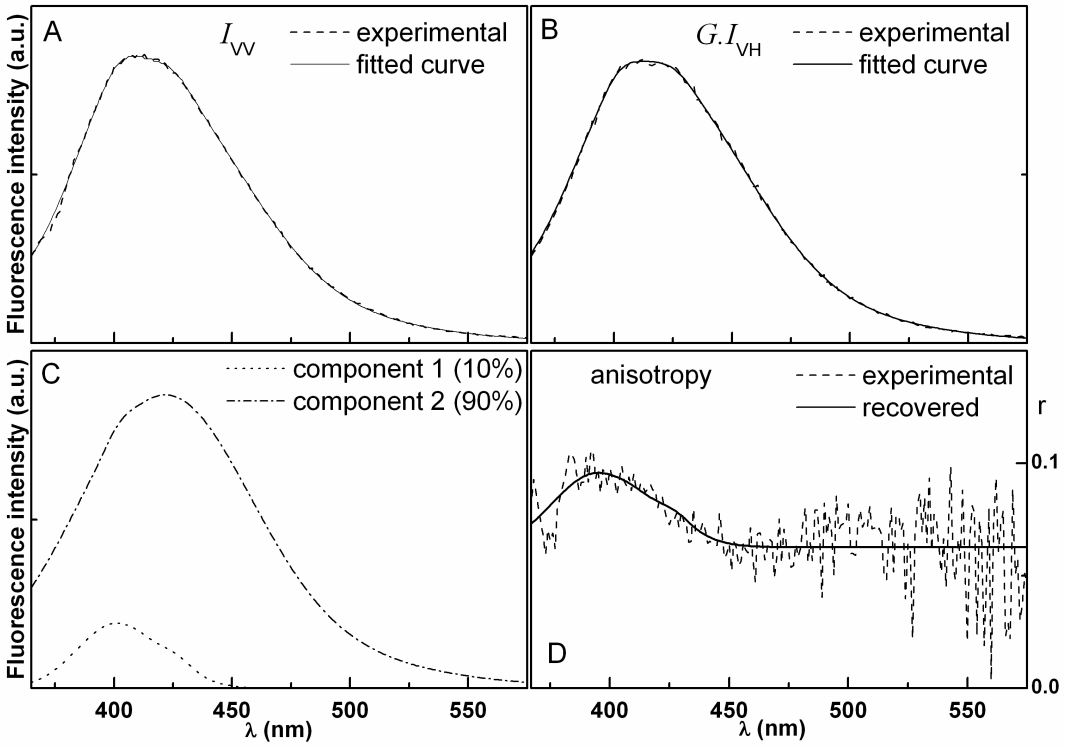


Figure 12. Fit of peptide **3** emission in DPPC/DPPG 3:1 lipid membranes (25 ºC). **A:** $I_{VV}$ component and fitted curve; **B:** $G{\cdot}I_{VH}$ component and fitted curve; **C:** Recovered spectral components from the fitting procedure; **D:** Fluorescence steady-state anisotropy and recovered curve (calculated from the recovered components).

Comparing the maximum wavelengths with the ones obtained for the emission in homogeneous solution (Figure 8 and Table 3), it can be concluded that component 1 with $\lambda_{max}$ = 402–405 nm corresponds to an environment similar to ethanol. This is the minor component (10% – 16%), attaining *ca.* 30% fraction in DPPC. The high anisotropy value, $r_1$, of this component points to a location inside the lipid bilayer, probably near the phospholipid polar head groups, feeling the transition to a more fluid phase at 55 ºC, above $T_m$ of both DPPC and DPPG. In general, the microviscosity of a lipid bilayer decreases from the interface to the interior of the membrane [38,39].

Table 5. Steady-state fluorescence anisotropy ($r$) of the two anisotropy components, respective maximum emission wavelengths ($\lambda_{max}$) and weight of the first component ($f_1$) for peptide **3** in lipid membranes. Fluorescence quantum yields are also indicated.

| **Lipid membrane composition** | **T (ºC)** | $f_1$ | $r_1$ | $\lambda_{1,max}$ **(nm)** | $r_2$ | $\lambda_{2,max}$ **(nm)** | $\Phi_F$ [a] |
|---|---|---|---|---|---|---|---|
| Neat DPPC | 25 | 0.26 | 0.241 | 402 | 0.052 | 431 | 0.035 |
| | 55 | 0.31 | 0.142 | 402 | 0.033 | 432 | 0.013 |
| DPPC/DPPG 3:1 | 25 | 0.10 | 0.242 | 402 | 0.063 | 422 | 0.031 |
| | 55 | 0.12 | 0.164 | 402 | 0.035 | 422 | 0.015 |
| DPPC/DPPG 1:1 | 25 | 0.14 | 0.222 | 404 | 0.046 | 424 | 0.023 |
| | 55 | 0.16 | 0.133 | 404 | 0.023 | 431 | 0.012 |
| DPPC/DPPG 1:3 | 25 | 0.11 | 0.191 | 402 | 0.066 | 421 | 0.030 |
| | 55 | 0.12 | 0.116 | 404 | 0.028 | 432 | 0.017 |
| Neat DPPG | 25 | 0.12 | 0.175 | 403 | 0.052 | 425 | 0.043 |
| | 55 | 0.20 | 0.089 | 405 | 0.028 | 435 | 0.020 |

[a] Relative to 9,10-diphenylanthracene in ethanol ($\Phi$ = 0.95 [19])

The major component, with maximum emission wavelength in the range 422–435 nm, corresponds to a hydrated environment, similar to pure water (Table 3). In fact, the anisotropy, $r_2$, is very low, pointing to a very fluid medium. Therefore, the RGD labelled peptide locates mainly in the outer part of the vesicle interfaces, in a medium with a fluidity approaching that of water. The fluorescence quantum yields of the peptide in lipid membranes (Table 5) are in accordance with this conclusion, as the values at room temperature are similar to the one measured in pure water (Table 3).

## Conclusions

The 3-(phenanthren-9-yl)-1*H*-indole-2-carboxylic acid (**2**) obtained from the cleavage of the methyl ester of the methyl 3-(phenanthren-9-yl)-1*H*-indole-2-carboxylate (**1**) was inserted in solid phase into a peptide containing the RGD sequence. The peptide was also prepared by solid phase synthesis using a Fmoc strategy and 2-chlorotrityl chloride resin.

Both phenanthrenyl-indole derivatives **1** and **2**, exhibit a solvent sensitive emission and generally high fluorescence quantum yields. The results point to the presence of a significant charge transfer mechanism in the excited state, especially for the compound with the carboxylic group.

Fluorescence measurements of the labelled peptide in solution showed a strong decrease in the fluorescence quantum yield, but a pH sensitive emission was detected.

The phenanthrenyl-indole derivatives and the labelled peptide were incorporated in lipid membranes of DPPC and/or DPPG. Steady-state fluorescence anisotropy measurements revealed that both indolic compounds are located inside the lipid bilayers and are able to report clearly the transition between the gel and liquid-crystalline phases. The RGD labelled peptide locates mainly in the outer part of the vesicle interfaces.

These results point to a promising utility of the phenanthrenyl-indole moiety as a fluorescence probe for biological systems, either as an extrinsic probe or as a label covalently bound to biomolecules.

## Acknowledgements

Fundação para a Ciência e a Tecnologia (FCT) – Portugal, QREN and program FEDER/COMPETE for financial support through Centro de Física (CFUM) and Centro de Química (CQ-UM) of University of Minho and through the research project PTDC/QUI/81238/2006, co-financed by FCT and FEDER/COMPETE (FCOMP-01-0124-FEDER-007467). FCT is also acknowledged for grants BII of B.F.H., PhD of G.P. (SFRH/BD/38766/2007) and post-Doc. of A.S.A. (SFRH/BPD/24548/2005). The NMR spectrometer Bruker Avance III 400 is part of the Portuguese NMR Network (Rede/1517/RMN/2005) which is also supported by the FCT.

## References

[1] J. B. A. Ross, A.G. Szabo, C.W.V. Hogue, *Fluoresc. Spectrosc.* **1997**, 278, 151–190.

[2] S. M. Twine, A.G. Szabo, *Methods Enzymol.* **2003**, 360, 104–127.

[3] A. R. Katritzky, T. Narindoshvili, *Org. Biomol. Chem.* **2009**, 7, 627-634.

[4] E. Pazos, O.Vázquez, J. L. Mascarenas, M. E. Vázquez, *Chem Soc. Rev.* **2009**, 38, 3348-3349.

[5] R. Dayam, F. Aiello, J. Deng, Y. Wu, A. Garofalo, X. Chen, N. Neamati, *J. Med. Chem.* **2006**, 49, 4526-4534.

[6] K-E. Gottschalk, H. Kessler, *Angew. Chem. Int. Ed.* **2002**, 41, 3767-3774.

[7] L. D. D'Andrea, A. Del Gatto, C. Pedone, E. Benedetti, *Chem. Biol. Drug Des.* **2006**, 67, 115-126.

[8] E. A. Murphy, B.K. Majeti, L.A. Barnes, M. Makale, S. Weis, K. Lutu-Fuga, W. Wrasidlo, D. Cheresh, *Proc. Natl. Acad. Sci. U. S. A.* **2008**, 105, 9343–9348.

[9] a) E. Garanger, D. Botutyn, J.L. Coll, M. Favrot, P. Dumy, *Org. Biomol. Chem.* **2006**, 4, 1958–1965; b) R.O. Hynes, *Cell* **1992**, 69, 11–25; c) P.C. Brooks, R.A. Clark, D.A. Cheresh, *Science* **1994**, 264, 569–571; d) R.O. Hynes, *Nat. Med.* **2002**, 8, 918–921.

[10] a) A. S. Abreu, E. M. S. Castanheira, P. M. T. Ferreira, L. S. Monteiro, G. Pereira, M-J. R. P. Queiroz, *Eur. J. Org. Chem.* **2008**, 5697-5703; b) G. Pereira, A. S. Abreu, E. M. S. Castanheira, P. J. G. Coutinho, P. M. T. Ferreira, M-J. R. P. Queiroz, *Eur. J. Org. Chem.* **2009**, 3906-3916; c) G. Pereira, E. M. S. Castanheira, P. M. T. Ferreira, M-J. R. P. Queiroz, *Eur. J. Org. Chem.* **2010**, 464-475.

[11] a) A. S. Abreu, N. O. Silva, P. M. T. Ferreira, M-J. R. P. Queiroz, *Tetrahedron Lett.* **2003**, 44, 3377-3379; b) A. S. Abreu, N. O. Silva, P. M. T. Ferreira, M-J. R. P. Queiroz, M. Venanzi, *Eur. J. Org. Chem.* **2003**, 4792-4796.

[12] S. Batzri, E. D. Korn, *Biochim. Biophys. Acta* **1973**, 298, 1015-1019.

[13] J. M. H. Kremer, M. W. J. v. d. Esker, C. Pathmamanoharan, P. H. Wiersema, *Biochemistry* **1977**, 16, 3932-3935.

[14] J. R. Nordlund, C. F. Schmidt, S. N. Dicken, T. E. Thompson, *Biochemistry* **1981**, 20, 3237-3241.

[15] B. R. Lentz, *Chem. Phys. Lipids* **1989**, 50, 171-190.

[16] J. S. Vincent, S. D. Revak, C. D. Cochrane, I. W. Levin, *Biochemistry* **1993**, 32, 8228-8238.

[17] J. N. Demas, G. A. Crosby, *J. Phys. Chem.* **1971**, 75, 991-1024.

[18] S. Fery-Forgues, D. Lavabre, *J. Chem. Educ.* **1999**, 76, 1260-1264.

[19] J. V. Morris, M. A. Mahaney, J. R. Huber, *J. Phys. Chem.* **1976**, 80, 969-974.

[20] J. R. Lakowicz, *Principles of Fluorescence Spectroscopy*, Kluwer Academic/Plenum Press, New York, **1999**.

[21] N. Mataga, T. Kubota, *Molecular Interactions and Electronic Spectra*, Marcel Dekker, New York, **1970**.

[22] D. Creed, *Photochem. Photobiol.* **1984**, 39, 537-562.

[23] B. Albinsson, M. Kubista, B. Nordén, E.W. Thulstrup, *J. Phys. Chem.* **1989**, 93, 6646-6654.

[24] H. Lippert, H.-H. Ritze, I.V. Hertel, W. Radloff, *Chem. Phys. Lett.* **2004**, 398, 526-531.

[25] I. Tatischeff, R. Klein, R. *Photochem. Photobiol.* **1975**, 22, 221-229.

[26] N. J. Turro, in *Modern Molecular Photochemistry*, Benjamin/Cummings Pub., Menlo Park (California), **1996**.

[27] M.-J. R. P. Queiroz, A. S. Abreu, E. M. S. Castanheira, P. M. T. Ferreira, *Tetrahedron* **2007**, 63, 2215–2222.

[28] M.-J. R. P. Queiroz, E. M. S. Castanheira, M. S. D. Carvalho, A. S. Abreu, P. M. T. Ferreira, H. Karadeniz, A. Erdem, *Tetrahedron* **2008**, 64, 382–391.

[29] E. M. S. Castanheira, A. S. Abreu, M. S. D. Carvalho, M.-J. R. P. Queiroz, P. M. T. Ferreira, *J. Fluorescence*, **2009**, 19, 501–509.

[30] D. R. Lide (Ed.), *Handbook of Chemistry and Physics*, 83$^{th}$ Edition, CRC Press, Boca Raton, **2002**.

[31] a) K. C. James, P. R. Noyce, *Spectrochim. Acta A* **1971**, 27, 691-696. b) G. R. Wileylb, S. I. Miller, *J. Am. Chem. Soc*. **1972**, 94, 3287-3293.

[32] *Gaussian 09, Revision A.02,* M. J. Frisch, G. W. Trucks, H. B. Schlegel, G. E. Scuseria, M. A. Robb, J. R. Cheeseman, G. Scalmani, V. Barone, B. Mennucci, G. A. Petersson, H. Nakatsuji, M. Caricato, X. Li, H. P. Hratchian, A. F. Izmaylov, J. Bloino, G. Zheng, J. L. Sonnenberg, M. Hada, M. Ehara, K. Toyota, R. Fukuda, J. Hasegawa, M. Ishida, T. Nakajima, Y. Honda, O. Kitao, H. Nakai, T. Vreven, J. A. Montgomery, Jr., J. E. Peralta, F. Ogliaro, M. Bearpark, J. J. Heyd, E. Brothers, K. N. Kudin, V. N. Staroverov, R. Kobayashi, J. Normand, K. Raghavachari, A. Rendell, J. C. Burant, S. S. Iyengar, J. Tomasi, M. Cossi, N. Rega, J. M. Millam, M. Klene, J. E. Knox, J. B. Cross, V. Bakken, C. Adamo, J. Jaramillo, R. Gomperts, R. E. Stratmann, O. Yazyev, A. J. Austin, R. Cammi, C. Pomelli, J. W. Ochterski, R. L. Martin, K. Morokuma, V. G. Zakrzewski, G. A.

Voth, P. Salvador, J. J. Dannenberg, S. Dapprich, A. D. Daniels, Ö. Farkas, J. B. Foresman, J. V. Ortiz, J. Cioslowski, and D. J. Fox, Gaussian, Inc., Wallingford CT, **2009**.

[33] F. Jensen, in *Introduction to Computational Chemistry*, John Wiley & Sons, West Sussex, England, **1999**.

[34] R. M. C. Dawson, D. C. Elliott, W. H. Elliott, K. M. Jones, *Data for Biochemical Research*, 3rd Edition, Oxford University Press, 1989.

[35] B. Valeur, *Molecular Fluorescence - Principles and Applications*, Wiley-VCH, Weinheim, **2002**.

[36] D. B. Siano, D. E. Metzler, *J. Chem. Phys.* **1969**, 51, 1856-1861.

[37] E. M. S. Castanheira, M. S. D. Carvalho, D. J. G. Soares, P. J. G. Coutinho, R. C. Calhelha, M.-J. R. P. Queiroz, *J. Fluorescence* **2010**, DOI: 10.1007/s10895-010-0607-3

[38] L. Tilley, K. R. Thulborn, W. H. Sawyer, *J. Biol. Chem.* **1979**, 254, 2592-2594

[39] M. A. Bahri, B. J. Heyne, P. Hans, A. E. Seret, A. A. Mouithys-Mickalad, M. D. Hoebeke, *Biophys. Chem.* **2005**, 114, 53-61.